Biosensors and Bioelectronics 197 (2022) 113759

Contents lists available at ScienceDirect

Biosensors and Bioelectronics

journal homepage: www.elsevier.com/locate/bios

Rapid detection of novel coronavirus SARS-CoV-2 by RT-LAMP coupled solid-state nanopores

Zifan Tang [a], Reza Nouri [a], Ming Dong [a], Jianbo Yang [b], Wallace Greene [b], Yusheng Zhu [b], Michele Yon [c], Meera Surendran Nair [c], Suresh V. Kuchipudi [c,d], Weihua Guan [a,e,*]

[a] Department of Electrical Engineering, Pennsylvania State University, University Park, PA, 16802, United States
[b] Department of Pathology and Laboratory Medicine, Penn State Hershey Medical, Hershey, PA, 17033, United States
[c] Animal Diagnostic Laboratory, Pennsylvania State University, University Park, PA, 16802, United States
[d] Center for Infectious Disease Dynamic, Pennsylvania State University, University Park, PA, 16802, United States
[e] Department of Biomedical Engineering, Pennsylvania State University, University Park, PA, 16802, United States

ARTICLE INFO

Keywords:
COVID-19
SARS-CoV-2
RT-LAMP
Solid-state nanopore
Clinical

ABSTRACT

The current pandemic of COVID-19 caused by SARS-CoV-2 (severe acute respiratory syndrome coronavirus-2) has raised significant public health concerns. Rapid and accurate testing of SARS-CoV-2 is urgently needed for early detection and control of the disease spread. Here, we present an RT-LAMP coupled glass nanopore digital counting method for rapid detection of SARS-CoV-2. We validated and compared two one-pot RT-LAMP assays targeting nucleocapsid (N) and envelop (E) genes. The nucleocapsid assay was adopted due to its quick time to positive and better copy number sensitivity. For qualitative positive/negative classification of a testing sample, we used the glass nanopore to digitally count the RT-LAMP amplicons and benchmarked the event rate with a threshold. Due to its intrinsic single molecule sensitivity, nanopore sensors could capture the amplification dynamics more rapidly (quick time to positive). We validated our RT-LAMP coupled glass nanopore digital counting method for SARS-CoV-2 detection by using both spiked saliva samples and COVID-19 clinical nasopharyngeal swab samples. The results obtained showed excellent agreement with the gold standard RT-PCR assay. With its integration capability, the electronic nanopore digital counting platform has significant potential to provide a rapid, sensitive, and specific point-of-care assay for SARS-CoV-2.

1. Introduction

Coronaviruses are enveloped positive-sense RNA viruses, which are commonly associated with acute respiratory infections in humans. In late December 2019, several local health facilities reported patients with pneumonia of unknown causes in Wuhan, Hubei Province, China (Zhu et al., 2020). The causative pathogen has been identified as a novel enveloped RNA betacoronavirus. Given the similarity to the previously isolated severe acute respiratory syndrome coronavirus (SARS-CoV), the new virus has been named SARS-CoV-2. This new virus causes coronavirus disease 2019 (COVID-19), and it was rapidly announced as a public health emergency of international concern by the World Health Organization (WHO). As of August 2021, there are a total of 198,778,175 confirmed cases, and 4,235,559 deaths of SARS-CoV-2 reported globally (WHO, 2020). In this pandemic of SARS-CoV-2, accessible, early, and accurate diagnosis is crucial to facilitate robust public health surveillance and rapid testing. The current gold-standard technique for SARS-CoV-2 testing is the reverse transcription-polymerase chain reaction (RT-PCR) (Udugama et al., 2020). Despite its high sensitivity and specificity, laboratory-based RT-PCR requires highly trained personnel, dedicated facilities, and instrumentations, thus limiting the testing capacity. To enhance the test accessibility, isothermal amplification techniques such as reverse transcription loop-mediated isothermal amplification (RT-LAMP) is widely studied as alternatives for COVID-19 testing (Thompson and Lei, 2020; Yan et al., 2020). The isothermal method has great potential as a point-of-care tool because it is a rapid, sensitive, and specific technique. During the early outbreak phase of the COVID-19 pandemic, a significant research effort focused on designing, validating, optimizing the RT-LAMP primers (Park et al., 2020; Yu et al., 2020). These efforts soon expanded to the scope of exploring alternative sample specimens (Azzi et al., 2020; Wyllie et al., 2020; Yelin et al., 2020) and simplifying the sample purification (Ning et al., 2021; Vogels

* Corresponding author. Department of Electrical Engineering, Pennsylvania State University, University Park, PA, 16802, United States.
E-mail address: w.guan@psu.edu (W. Guan).

https://doi.org/10.1016/j.bios.2021.113759
Received 16 August 2021; Received in revised form 25 September 2021; Accepted 29 October 2021
Available online 2 November 2021

et al., 2021). In addition, the CRISPR based detection has been incorporated with the RT-LAMP to improve its specificity performances (Wang et al., 2021), and the high-throughput sequencing has been incorporated with the RT-LAMP (LAMP-sequencing) to facilitate population-level of usage (Thi et al., 2020).

The results of the RT-LAMP amplification are often read out using different optical methods, such as changes in turbidity caused by magnesium pyrophosphate precipitate (Mori et al., 2004), changes in fluorescence using dyes (Ganguli et al., 2020; Roy et al., 2016; Sun et al., 2020), colorimetric pH indicators (Wei et al., 2021; Yu et al., 2020), or gel electrophoresis followed by UV detection (Lamb et al., 2020). Each of these methods would require a minimum concentration of the signaling reporters (c_{min}) for the readout system to distinguish between positives and negatives. Depending on different readout systems (*e.g.*, naked eye (Thi et al., 2020) versus highly sensitive fluorescence detector (Ning et al., 2021; Yan et al., 2020)), the c_{min} could range from mM to nM. This required minimal signaling reporter concentration can be linked to the time to positive (TTP) as $c_{min} = TTP \times v_r$, in which v_r is the average reaction rate of the assay. It is evident that reducing the detection c_{min} is preferred towards quick time to positive. In this regard, the intrinsic single-molecule sensitivity of nanopore sensors (Albrecht, 2019; Miles et al., 2013) is highly intriguing since it enables a significantly reduced c_{min} and thus reduce the time required for making the positive/negative call. Existing works on nanopores have demonstrated that nanopores can easily capture the analyte at the pM range (Albrecht, 2019; Nouri et al., 2019). Our previous work has demonstrated a LAMP-coupled nanopore sensor for malaria nucleic acid test (Tang et al., 2019). The integration and miniaturization potential of the label-free, electronics-based nanopore sensors could open a new avenue for enhancing the accessibility of the molecular testing at the point of care.

In this study, we report an RT-LAMP coupled nanopore platform for rapid detection of SARS-CoV-2. We compared the time to positive and sensitivity performances of two one-pot RT-LAMP assays targeting the nucleocapsid and envelop genes. For qualitative positive/negative classification of a testing sample, the nanopore sensor was used to measure the amplicon size and concentration by the digital counting method. Thanks to its intrinsic single molecule sensitivity, the nanopore sensor could make a faster positive/negative call than bulk optical methods. We validated this method with both spiked saliva samples and COVID-19 clinical nasopharyngeal swab samples. With 127 clinical samples and RT-PCR as the gold standard, our nanopore platform was able to detect SARS-CoV-2 with 98% diagnostic sensitivity, and 92% diagnostic specificity. We believe the RT-LAMP coupled electronic nanopore digital counting platform has significant potential to provide a rapid, sensitive, and specific detection of SARS-CoV-2.

2. Results and discussion

2.1. Overall workflow from sample to nanopore counting

Fig. 1 illustrates the overall workflow of the platform from sample collection to RT-LAMP coupled nanopore detection. The SARS-CoV-2 viral RNA was firstly extracted and purified from either the nasopharyngeal swab sample (Butler-Laporte et al., 2021; Wyllie et al., 2020; Yelin et al., 2020) or the saliva sample (Azzi et al., 2020; Butler-Laporte et al., 2021; Nagura-Ikeda et al., 2020; Vogels et al., 2021) (Fig. 1a). A subsequent isothermal RT-LAMP amplification was performed at 65 °C. In the presence of a few copies of SARS-CoV-2 viral RNA, a dumbbell-like DNA structure will be synthesized as a template for further amplification. The final product obtained from the RT-LAMP reaction is a mixture of stem-loop DNAs with various stem lengths and various cauliflower-like structures with multiple loops (Fig. 1b), formed by annealing between alternately inverted repeats of the target sequence in the same strand (Tomita et al., 2008). Typically, amplicons can be amplified as much as 10^9 times within an hour (Parida et al., 2008).

Afterward, the nanopore counting analysis was performed to examine the concentration of the resulting amplicons. This is based on the fact that the nanopore event rate has a linear relation with the

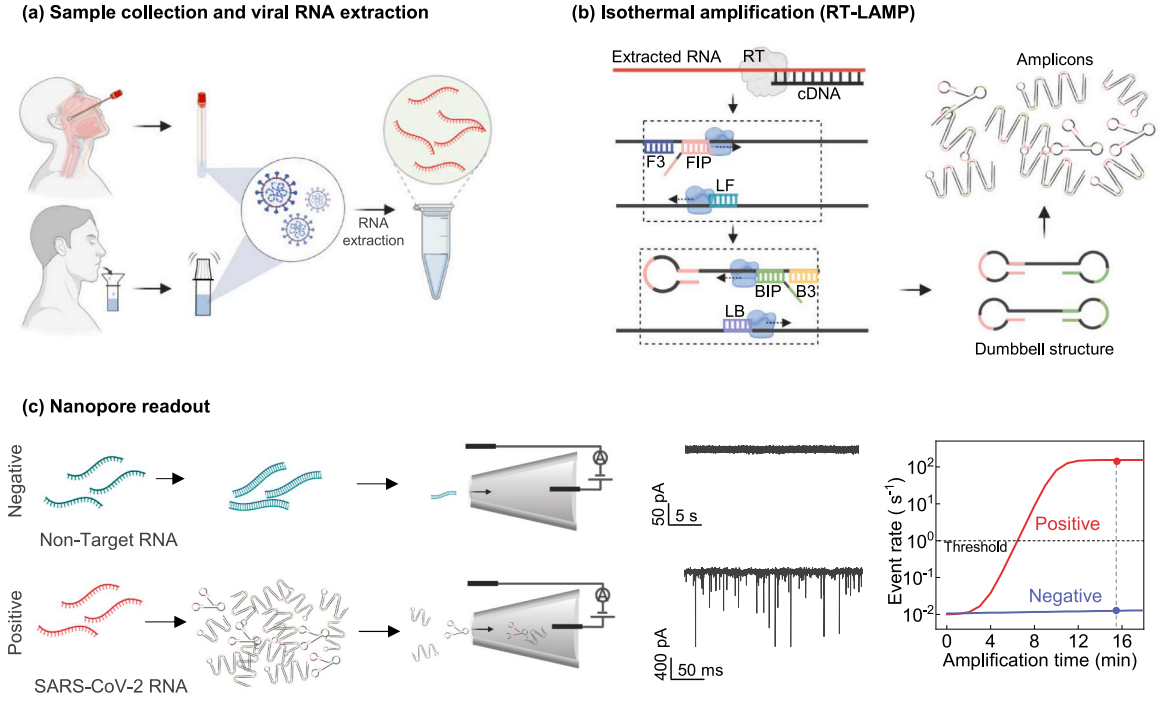

Fig. 1. Workflow of RT-LAMP coupled nanopore method for SARS-CoV-2 detection. (a) Sample collection, preparation, and RNA extraction from either the nasopharyngeal swab sample or the saliva sample. (b) RT-LAMP amplification. One step RT-LAMP reaction is performed at 65°C for 15 min. (c) Nanopore readout. In a negative control sample, no amplification occurs, resulting in a negligible event rate. In a positive case, amplicons increased significantly, resulting in a sharp increase in event rate. The right panel shows the nanopore event rate as a function of RT-LAMP reaction time. The event rate threshold was set at $1s^{-1}$ as the criteria for a positive call.

analyte concentration in the diffusion-limited region (Nouri et al., 2019; Tang et al., 2019). Fig. 1c shows two representative cases: a non-target negative control and a positive sample. For the negative control sample, no amplification would occur, resulting in an unchanged product concentration. We found the nanopore event rate for the negative control is negligible ($<0.029\ s^{-1}$ at 99.7% confidence level, Fig. S1) after 15 min of reaction. This ultra-low event rate suggests that the background molecules in the RT-LAMP master mix will not interfere with the nanopore analysis of amplicons. On the other hand, the event rate for the positive sample increased significantly to $110\ s^{-1}$. This result indicates that amplicons concentration indeed increased after 15 min of reaction, and the concentration change can be clearly captured by our nanopore event rate. The right panel of Fig. 1c shows the nanopore event rate as a function of RT-LAMP reaction time. We adopted an event rate threshold of $1\ s^{-1}$ as the criteria for a positive call in our study unless otherwise stated. This threshold is much higher than the background event rate in the negative control ($<0.029\ s^{-1}$) such that the false-positive rate can be minimized.

2.2. SARS-CoV-2 RT-LAMP assay validation

We first validated the RT-LAMP assay against the SARS-CoV-2 RNA. We adopted two LAMP primer sets targeting the N and E gene of SARS-CoV-2, respectively (Broughton et al., 2020). Table S1 and Table S2 summarized the primer information and the RT-LAMP reaction setup. Fig. 2a&b presented the triplicated real-time RT-LAMP results on a 10 × serial dilution of heat-inactivated SARS-CoV-2 RNA samples (stock concentration: 2×10^5 copies/μl) using a benchtop PCR instrument. As shown in Fig. 2c, the N primer set showed a better performance than the E primer set in terms of sensitivity and speed. The E primer set was not able to pick up 20 copies per reaction, while the N primer set can detect 2 out of 3 replicates at 20 copies. Moreover, the time to positive (TTP) value of N primer set was less than 10 min for all input concentrations, whereas E primer set took more than 13 min even for the most concentrated case (2×10^5 copies).

Based on this comparison, we chose the N primer set for our SARS-CoV-2 RT-LAMP assay in the following studies. To determine the limit of detection (LoD) of this assay, we performed the real-time RT-LAMP

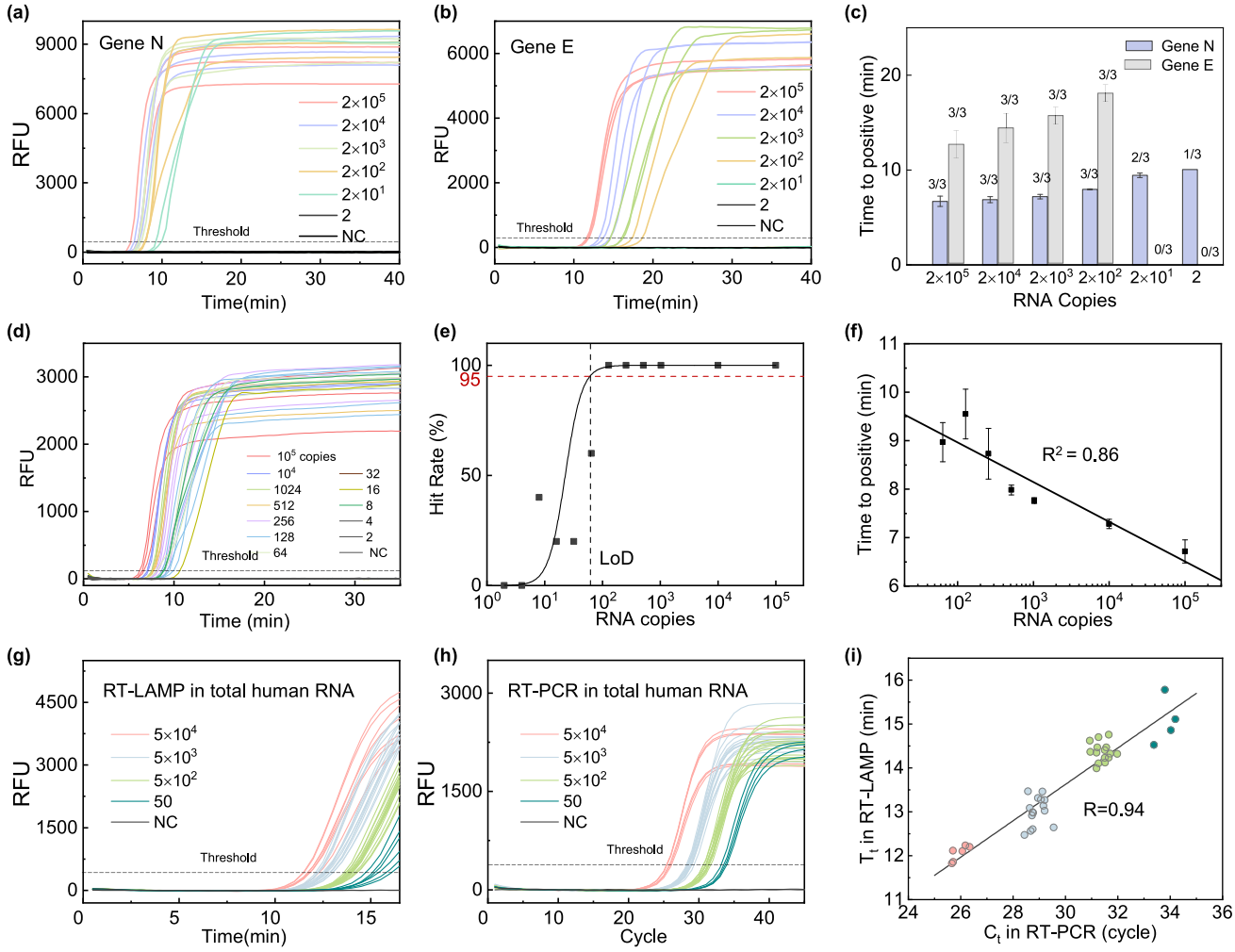

Fig. 2. RT-LAMP assay validation. (a) N primer set results, and (b) E primer set results with viral RNA concentrations ranging from 2 and 10^5 copies per reaction. (c) Time to positive value comparison between the N primer set (blue bars) and the E primer set (grey bars) at different RNA concentrations. The N primer set showed better performances in terms of sensitivity and time to positive. (d) Real-time RT-LAMP result with a finer serial dilution (2 ×) using N primer set. (e) The extracted hit rate at various RNA concentrations to establish the assay LoD, which is determined to be 65 copies at 95% confidence level. (f) Time to positive value with N primer sets at concentrations ranging between 10^2 and 10^5 copies per reaction. A good linearity is obtained, indicating that a semi-quantitative test is feasible. (g) Real-time RT-LAMP result in saliva RNA background. (h) Real-time RT-PCR result in saliva RNA background. (i) The correlation between the RT-PCR and RT-LAMP measurement in total saliva RNA background. (For interpretation of the references to color in this figure legend, the reader is referred to the Web version of this article.)

reaction with a 2 × serially diluted RNA sample down to 2 copies. As shown in Fig. 2d, concentrations above 128 copies/reaction were all amplified successfully, and concentrations below 4 copies/reaction were not able to be picked up. To estimate the assay LoD, we fitted a logistic curve for the hit rates at different RNA copies (Holstein et al., 2015). The hit rate is defined as the number of amplified samples over all samples. As shown in Fig. 2e, the LoD of the N primer set RT-LAMP assay is determined to be 65 copies/reaction at the 95% confidence level. This LoD is on par with other reported RT-LAMP assays targeting N regions (Rodriguez-Manzano et al., 2021; Thi et al., 2020; Thompson and Lei, 2020). In addition, we also examined the threshold time as a function of the RNA concentrations. As shown in Fig. 2f, the threshold time decreased from 10 min to 7 min when the RNA concentration increased from 2 to 10^5 copies. A linear fit produced the R^2 with 0.86, indicating that a semi-quantitative RT-LAMP test is feasible.

To evaluate the effectiveness of RT-LAMP assay in human total RNA background and benchmark it with the gold standard RT-PCR assay from United States CDC (Table S3), we prepared 10-fold serial dilutions of SARS-CoV-2 RNAs in human total RNA background. The human total RNA was extracted from healthy saliva samples by a commercial kit. The final concentration of salivary RNA measured by the Nanodrop was 87 ng/μl. A total of 42 samples at four different concentrations were tested. Fig. 2g and h showed the RT-LAMP and RT-PCR results, respectively. As shown in Fig. 2i, the RT-LAMP threshold time and the RT-PCR threshold cycle showed a Pearson correlation coefficient of 0.94, indicating an excellent quantitative agreement between RT-LAMP and RT-PCR results, despite the human total RNAs background.

2.3. Nanopore counting of RT-LAMP amplicons

After validating the SARS-CoV-2 RT-LAMP assay, we set out to perform the nanopore counting analysis on the resulting amplicons. A testing sample with an RNA concentration of 10^4 copies was amplified for different reaction times ranging from 0 to 16 min. The reaction was stopped by heating the reaction to 95 °C for 5 min. The end products were examined by gel electrophoresis. As shown in Fig. 3a, the gel started to show a typical ladder pattern with many bands of different sizes after 8 min of RT-LAMP reaction. These bands became darker as the reaction times increased, indicating a successful amplification occurred.

These end products were then examined by the glass nanopore sensor. The amplicon solution was adjusted to 1M salt concentration to facilitate the nanopore measurement (Nouri et al., 2019). A typical nanopore readout was performed under 200 mV bias until at least 100 events were detected or 30 min of measurement was reached. A minimal event number of 100 ensures <10% uncertainty of event rate determination (Nouri et al., 2019). Fig. 3b presents the representative current traces of amplicons at different reaction times (note scale differences). It is evident that more events showed up as we increased the reaction time. To perform the nanopore counting, we first characterized the events by their current drop (ΔI) and dwell time (Δt). As shown in Fig. 3c, there is a clear population shift in the ΔI *vs.* Δt scattering plot, indicating the distribution change of the amplicon size. This shift is expected since the LAMP product is a mixture of stem-loop DNA with various stem lengths and various cauliflower-like structures with multiple loops (Parida et al., 2008; Tomita et al., 2008).

To quantify the amplicon size distributions and their relative abundance, we used the event charge deficit (ECD, defined as $\int_{\Delta t} \Delta I(t)dt$) to represent the approximate amplicon size (Fologea et al., 2007). An ECD bin size of 20 fC was used to characterize each subpopulation. The event rate of the ECD sub-population was obtained by normalizing the corresponding event numbers by the nanopore measurement time. This normalization process gives us the capability to benchmark nanopore measurements performed with different readout times. Fig. 3d shows the distribution of event rate *vs.* ECD at different reaction times. Two interesting features can be observed. First, the event rate of all sub-populations increases as the amplification time increases. For instance, the event rate for ECDs below 20 fC was 0.016 s^{-1} at 0 min and increased to 129.50 s^{-1} at 16 min. The event rate for ECDs between 400 and 420 fC was 0 s^{-1} at 0 min and increased to 0.25 s^{-1} at 16 min. This change indicates the amplicon concentration of each size increased, and the RT-LAMP product was dominated by smaller amplicons (note the log scale in rate in Fig. 3d). Second, the sub-populations with ECD >60 fC started to be captured by the nanopore measurement after 6 min of reaction. The event rate of the sub-populations increased about 10 times compared to 0 min. However, gel electrophoresis analysis (Fig. 3a) was

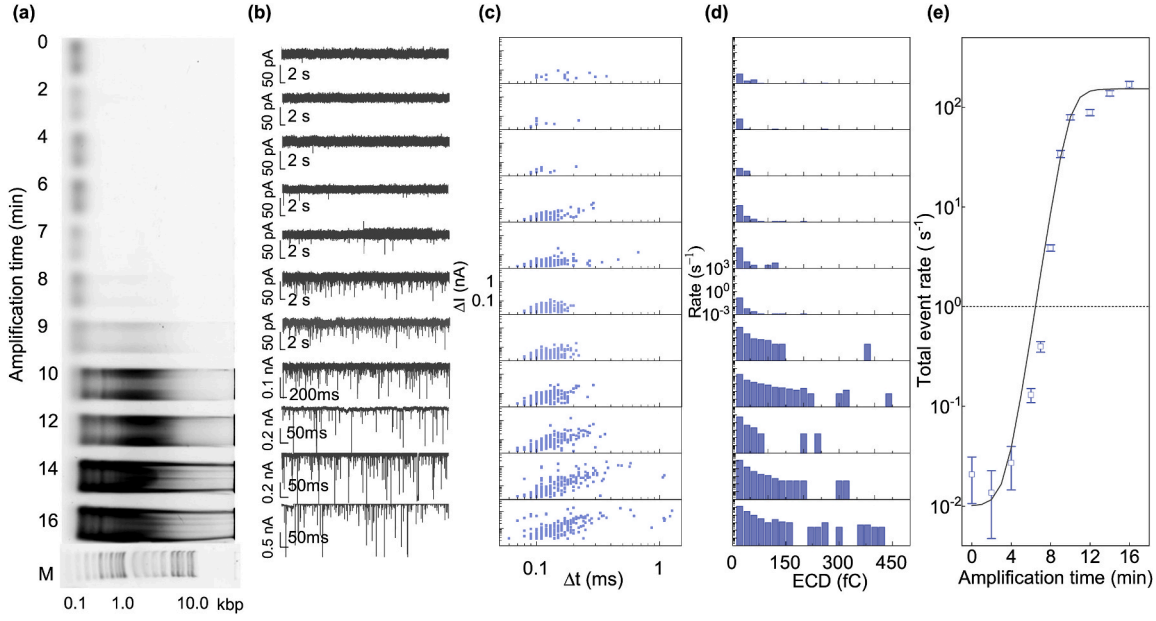

Fig. 3. Nanopore counting of RT-LAMP amplicons. (a) Gel electrophoresis (2% agarose gel) result of the RT-LAMP products, at various reaction times from 0 min to 16 min. (b) Corresponding current time traces measured in nanopores with 200 mV bias (Note the scale differences). (c) Corresponding current drop *vs*. dwell times distribution at different reaction times. (d) Corresponding event rate distribution as a function of ECD values. (e) The total event rate as a function of the reaction time. The solid line is fitting to the logistic growth model $R^2 = 0.95$.

not able to distinguish the population increase at the same conditions, only weak bands starting to be visible after 8 min of reaction. This suggested that the nanopore readout is more sensitive than the gel analysis, and nanopore measurement can capture the amplification dynamic faster.

We further analyzed the total event rate by the summation of all sub-populations event rates ($R_{tot} = \sum_i R_i$). As shown in Fig. 3e, the total event rate increased more than three orders of magnitude from 0.021 s^{-1} to 168.23 s^{-1} as the reaction time went from 0 min to 16 min. We fitted the total event rate as a function of RT-LAMP reaction time by the logistic growth model (Subramanian and Gomez, 2014; Tang et al., 2019) with $R(t) = R_L + (R_H - R_L)/(1 + e^{-\beta(t-t_0)})$, where R_L (0.01 s^{-1}) and R_H (152.8 s^{-1}) are the low and high bound of the event rate, t_0 (9.94 min) is the time when the growth rate is at maximum, and β (1.45 min^{-1}) is the maximum steepness of amplification rate. The fitted R_L value of 0.01 s^{-1} was close to the event rate of 9 negative controls ($\mu+3\sigma$ = 0.029 s^{-1}, Fig. S1), where mean (μ) and standard deviation (σ) of the event rate is 0.009 s^{-1} and 0.007 s^{-1} respectively. It is worth mention that choosing a proper threshold for making a positive/negative call is a trade-off between turnaround time and specificity. For example, if we set the threshold based on the negative controls (0.029 s^{-1}), a positive decision can be made in 5 min, but it may lead to a high false-positive rate. In this study, we set a threshold of 1 s^{-1} (100 times higher than the R_L) to minimize the false positive rate.

2.4. Evaluation with spiked saliva samples

We evaluated the nanopore sensor analytical sensitivity using the SARS-CoV-2 spiked saliva sample. These spiked saliva samples were prepared by adding 2-fold serially diluted heat-inactivated SARS-CoV-2 RNA into the total RNA background extracted from the healthy saliva samples. The final viral RNA concentrations range from 10^5 copies/μl to 10 copies/μl. The RT-LAMP reactions were performed with 1 μl of the viral RNA sample at 65°C for 15 min (Fig. S2), followed by the nanopore counting for event rate determination. Each concentration was tested at least three times. The limit of detection was established as the lowest number of concentrations that >95% percent sample was tested positive. Fig. 4a shows the measured event rate as a function of different SARS-CoV-2 RNA concentrations. As shown, at the concentration of 100 copies/μl, 5 out 5 samples were determined to be positive since all have event rates larger than 1 s^{-1}, whereas 2 out 5 samples at the concentration of 50 copies/μl were detected as positives. The LoD was thus determined to be 100 copies/μl with the SARS-CoV-2 spiked saliva sample. This LoD with saliva RNA in the background is similar to the LoD obtained by testing the purified viral RNA sample (65 copies/μl, Fig. 2e). These results confirmed that (1) the RT-LAMP assay is specific to the SARS-CoV-2 RNA, and (2) the saliva RNA background has negligible impact on event rate determination since SARS-CoV-2 RNA specific amplicons dominated the RT-LAMP product.

For the analytical specificity test, we used three different human coronaviruses (229E, NL63, and OC43) RNAs spiked in the saliva RNA background. We tested five replicates, each at the concentration of 10^5 copies/μl. As shown in Fig. 4b, a sharp contrast between the event rates of SARS-CoV-2 and other human coronavirus samples can be observed. The average event rate of SARS-CoV-2 cases was 110 s^{-1}, and the average event rate of the 229E, NL63, and OC43 was 0.03 s^{-1}, 0.01 s^{-1}, and 0.05 s^{-1}, respectively. The *t*-test showed that the event rate of the SARS-CoV-2 samples is statistically significant compared to the other three human coronaviruses samples. This result confirmed an excellent analytical specificity of the RT-LAMP coupled nanopore sensor against the SARS-CoV-2.

2.5. Clinical validation with nasopharyngeal swab samples

To evaluate the utility of the nanopore sensor against real clinical samples, we tested a total of 127 nasopharyngeal swab clinical samples obtained from Penn State Hershey Medical Center. These clinical samples were coded to remove information associated with patient identifiers. The FDA EUA-Authorized RT-PCR with Simplexa COVID-19 Direct assay (DiaSorin Molecular, Cypress, CA, USA) performed at initial diagnosis is considered the reference method to benchmark our nanopore sensors. A total of 50 positive and 77 negative samples were tested. The viral RNAs from these clinical samples were firstly extracted by ThermoFisher MagMAX™ Viral/Pathogen Nucleic Acid Isolation Kit. We then performed the RT-LAMP reactions at 65°C for 15 min and measured event rates of the products by nanopore counting (Fig. 5a). As shown, it is clear that the event rate of positives was significantly higher than that of the negatives ($p < 0.00001$). With a predefined event rate threshold of 1 s^{-1}, 49 out of 50 positives were detected as true positives, and 70 out of 77 negatives were detected as true negatives (Table 1). The diagnostic sensitivity, and specificity of the nanopore sensor compared

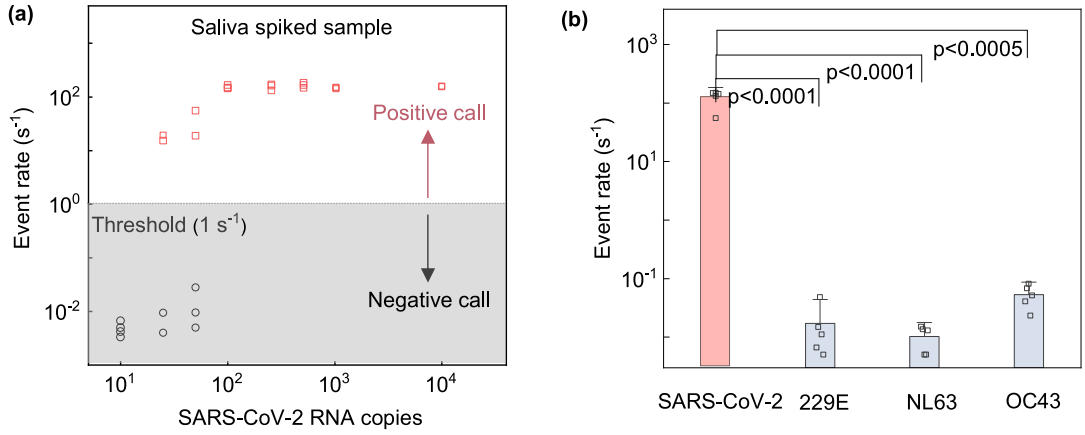

Fig. 4. Analytical sensitivity and specificity test with saliva spiked sample. (a) Event rate of the RT-LAMP amplicons at various concentrations of SARS-CoV-2 in total saliva RNA background. A event threshold of 1 s^{-1} is used for positive/negative call. (b) The event rate for SARS-CoV-2 and three other non-SARS-CoV-2 targets with a concentration of 10^5 copies in total saliva RNA background. All non-SARS-CoV-2 targets showed event rates much less than 1 s^{-1} and were correctly classified as negatives.

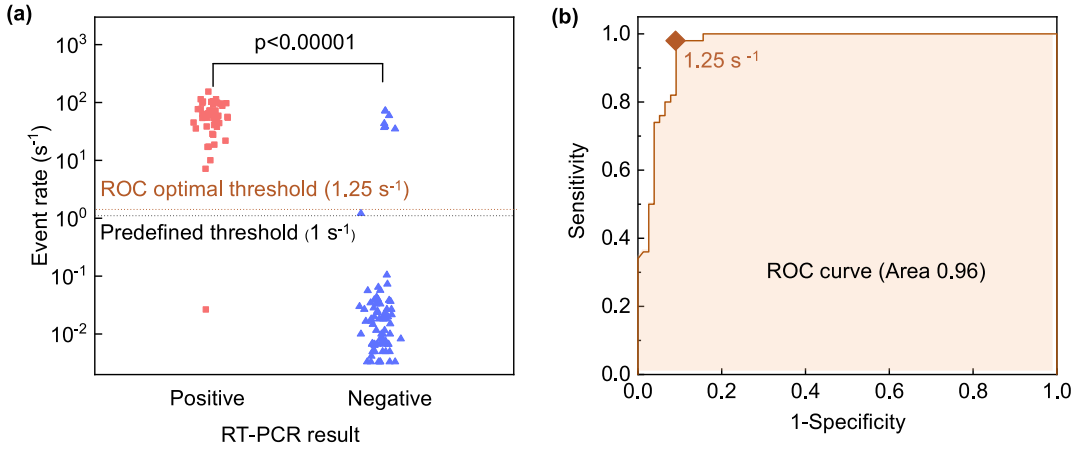

Fig. 5. Diagnostic sensitivity and specificity test with clinical nasopharyngeal swab samples. (a) Event rate of the RT-LAMP amplicons for a total of 127 samples. These samples were initially tested with RT-PCR (50 positives and 77 negatives). A predefined event rate threshold of 1 s^{-1} and a ROC optimized event rate threshold of 1.25 s^{-1} were used in nanopore sensors to classify the samples. (b) ROC curve analysis of the test result. The area under the ROC curve (AUC) is 0.96.

Table 1
Statistics of RT-LAMP coupled nanopore sensor for analyzing 127 clinical nasopharyngeal swab samples.

Nanopore result	Pos/ Pos	Neg/ Pos	Pos/ Neg	Neg/ Neg	Sensitivity (95%CI)	Specificity (95%CI)
Predefined threshold	49/ 50	1/50	7/77	70/ 77	98.0% (94.1–100)	90.9% (84.5–97.3)
ROC threshold	49/ 50	1/50	6/77	71/ 77	98.0% (94.1–100)	92.2% (86.2–98.2)

to the reference method was 98% (95% CI = 94.1%–100%) and 90.9% (95% CI = 84.5%–97.3%).

We further evaluated the receiver operating characteristic (ROC) curve (Bewick et al., 2004; Zweig and Campbell, 1993) to find the optimal event rate threshold for positive/negative cutoff by varying the threshold from 0.001 to 500 s^{-1} (Fig. 5b). As shown, increasing the event rate threshold will improve the diagnostic specificity but deteriorates the diagnostic sensitivity. The optimal event rate threshold corresponds to the case where both the specific and sensitivity is closest to 1 (Bewick et al., 2004; Zweig and Campbell, 1993). Based on this approach, we obtained the ROC optimal event rate threshold as 1.25 s^{-1}. Note that the optimal threshold is highly relevant to the sample set. With this optimized threshold, the testing statistics were re-assessed and summarized in Table 1. As shown, the statistics using the ROC threshold are very similar to those with a predetermined threshold of 1 s^{-1}. The area under curve (AUC) was measured to be 0.96, indicating the RT-LAMP coupled nanopore sensor is highly sensitive and specific against SARS-CoV-2.

3. Conclusion

In summary, we have demonstrated a highly sensitive, specific, and rapid SARS-CoV-2 detection platform by coupling the RT-LAMP with glass nanopore sensors. The optimized RT-LAMP assay targeting the nucleocapsid gene showed an LoD of 65 copies at the 95% confidence level. It also possessed an excellent specificity against other human coronavirus RNA targets. The nanopore digital counting method was able to pick up the amplification process much quicker than the bulk optical method due to its intrinsic single molecule level of sensitivity. Validation of the nanopore platform with 127 clinical nasopharyngeal swab samples demonstrated its excellent diagnostic performances using RT-PCR as the gold standard. With further integration of the electronics and miniaturization of the device, RT-LAMP coupled nanopore digital counting method has great potential for developing next-generation point of care molecular diagnostics for diseases such as COVID-19.

4. Methods

4.1. Materials and chemicals

Quartz capillary with inner and outer diameter of 0.5 and 1 mm was purchased from Sutter Instrument. Pipette holder (QSW-T10N) and 0.2 mm Ag wire was purchased from Warner Instruments. Micro-injector with 34 gauge was purchased from World Precision Instruments. KCl and Tris-EDTA-buffer solution (pH 8.0) were purchased from Sigma-Aldrich. All solutions were filtered with a 0.2 μm syringe filter (Whatman). Mineral oil was purchased from Sigma-Aldrich. Heat-inactivated SARS-CoV-2 (ATCC® VR-1986HK™) RNA was purchased from ATCC. Synthetic human coronavirus 229E RNA (103011), NL63 RNA (103012) and 229E RNA (103013) were purchased from Twist Bioscience. QIAamp Viral RNA Kit was purchased from Qiagen. ThermoFisher MagMAX Viral/Pathogen Nucleic Acid Isolation Kit was purchased from ThermoFisher.

4.2. Glass nanopore fabrication and characterization

The quartz capillaries with inner and outer diameters of 0.5 and 1 mm were first cleaned by piranha for 30 min to remove any organic contaminants, then repeatedly rinsed with DI water and dried in an oven at 100 °C for 15 min. A laser pipette puller (P-2000, Sutter Instruments, USA) was used to fabricate the nanopore using a two-line program: (1) Heat 750, Filament 5, Velocity 50, Delay140, and Pull 50; (2) Heat 715, Filament 4, Velocity 30, Delay 145, and Pull 225. This recipe typically produces nanopore size around 10 nm (Fig. S1).

4.3. Nanopore sensing and data analysis

The glass nanopore was held by a pipette holder and immersed in a PCR tube, forming the *cis* and *trans* chambers. Micro-injector with 34 gauge was used to inject the solution into the nanopore, and both sides of the chambers were filled with 1 M KCl. Two Ag/AgCl electrodes were inserted into the KCl solution. A typical voltage of 200 mV was applied across the nanopore constriction with a 6363 DAQ card (National Instruments, USA). The ionic current traces were amplified by Axopatch 200B (Molecular Device, USA), low-pass filtered at 10 kHz, and

digitalized by the 6363 DAQ. The data was acquired by a customized LabVIEW software (National Instruments, USA). The nanopore measurement system was inside a homemade Faraday cage to shield the environmental noise. A custom-built MATLAB (MathWorks, USA) program was developed to analyze the current drop, duration time, ECD, and event rate.

4.4. SARS-CoV-2 RT-PCR

We used the United States CDC primer sets targeting the N1 region of the SARS-CoV-2 (Table S3). The 20 μl of the RT-PCR reaction mix consists of 5 μl of the RNA template, 1.5 μl of primer mix (50 μM forward primer, 50 μM reverse primer, 20 μM probes), 10 μl of qScript™ XLT One-Step RT-qPCR Tough Mix (2X), and 3.5 μl of H_2O. The RT-PCR process was performed for 45 cycles in the Bio-Rad CFX96 Real-Time PCR system. Each cycle consists of 3 s denaturation step at 95 °C and 30 s annealing step at 55 °C.

4.5. SARS-CoV-2 RT-LAMP

The total volume of the RT-LAMP assays contains a 24 μl master mix and 1 μl RNA sample. The master mix includes isothermal buffer, PCR grade H_2O, $MgSO_4$ (7 mM), Styo-9 green (0.5 μM), deoxyribonucleotide triphosphates (dNTPs, 1.4 mM), Bst 2.0 DNA polymerase (0.4 U/μl), Warmstart reverse transcriptase (0.3 U/μl), primer sets (0.2 mM F3 and B3c, 1.6 mM FIP and BIP, 0.8 mM LF and LB, see Table S1 for primer design). Table S2 summarized the RT-LAMP recipe. The reaction was performed at a constant temperature of 65°C using either a benchtop PCR instrument (Bio-Rad CFX96) or a customized heat block. All the reactions were added with an additional 25 μl mineral oil to prevent evaporation and cross-contamination.

4.6. Spiked saliva sample testing

The saliva samples were collected from healthy volunteers. The saliva RNAs were extracted by the QIAamp Viral RNA Mini Kit according to the manufacturer protocol. The final concentration of extracted RNA was measured by Nanodrop (Thermo Fisher Scientific) as 87 ng/μl. The heat-inactivated SARS-CoV-2 RNAs and non-SARS-CoV-2 human coronavirus synthetic controls were spiked into the extracted saliva RNA solution at various concentrations ranging from 10 to 10^5 copies/μl. Typically 1 μl of the mock RNA sample was used in the reaction unless otherwise stated.

4.7. Clinical nasopharyngeal sample testing and statistical analysis

Nasopharyngeal swab samples were obtained from the Penn State Milton S. Hershey Medical Center in Hershey, PA at various times from October 2020 to February 2021. The use of these deidentified specimens was approved by the institutional review board (IRB) of the Pennsylvania State University Hershey Medical Center (study number STUDY00016633). All these nasopharyngeal swab samples were initially tested with the FDA EUA-Authorized Simplexa RT-PCR COVID-19 Direct assay (DiaSorin Molecular, Cypress, CA, USA). The collected nasopharyngeal samples were stored in the viral transport medium (VTM) and frozen at −80°C before use. The viral RNAs were extracted by ThermoFisher MagMAX™ Viral/Pathogen Nucleic Acid Isolation Kit in the Animal Diagnostic Laboratory (BSL 3) at Penn State, University Park in accordance with a protocol approved by the Institutional Biosafety Committee. The diagnostic sensitivity is defined as TP/(TP + FN). The diagnostic specificity is defined as TN/(TN + FP). TP, TN, FP, FN represents true positive, true negative, false positive, and false negative, respectively.

Notes

The authors declare no competing financial interest.

CRediT authorship contribution statement

Zifan Tang: designed and performed the RT-PCR, fabricated the nanopores, designed and performed the RT-LAMP coupled nanopore sensing experiment, Writing – original draft, co-wrote the manuscript, with discussion from all authors. **Reza Nouri:** designed and performed the RT-PCR. **Ming Dong:** fabricated the nanopores, with discussion from all authors. **Jianbo Yang:** collected the clinical nasopharyngeal swabs and performed the initial clinical study. **Wallace Greene:** collected the clinical nasopharyngeal swabs and performed the initial clinical study. **Yusheng Zhu:** collected the clinical nasopharyngeal swabs and performed the initial clinical study. **Michele Yon:** extracted the viral RNA from nasopharyngeal swab samples. **Meera Surendran Nair:** extracted the viral RNA from nasopharyngeal swab samples. **Suresh V. Kuchipudi:** extracted the viral RNA from nasopharyngeal swab samples. **Weihua Guan:** Conceptualization, and, Supervision, Writing – original draft, co-wrote the manuscript, with discussion from all authors.

Declaration of competing interest

The authors declare that they have no known competing financial interests or personal relationships that could have appeared to influence the work reported in this paper.

Acknowledgments

This work is supported by the National Science Foundation under Grant No. 2045169. The content is solely the responsibility of the authors and does not necessarily represent the official views of the National Science Foundation. W.G. and S.V.K acknowledges the seed funding from PennState Huck Institutes of the Life Sciences & Materials Research Institute for interdisciplinary virus research.

Appendix A. Supplementary data

Supplementary data to this article can be found online at https://doi.org/10.1016/j.bios.2021.113759.

References

Albrecht, T., 2019. Single-molecule analysis with solid-state nanopores. Annu. Rev. Anal. Chem. 12, 371–387.

Azzi, L., Carcano, G., Gianfagna, F., Grossi, P., Dalla Gasperina, D., Genoni, A., Fasano, M., Sessa, F., Tettamanti, L., Carinci, F., 2020. Saliva is a reliable tool to detect SARS-CoV-2. J. Infect. 81 (1), e45–e50.

Bewick, V., Cheek, L., Ball, J., 2004. Statistics review 13: receiver operating characteristic curves. Crit. Care 8 (6), 508.

Broughton, J.P., Deng, X., Yu, G., Fasching, C.L., Servellita, V., Singh, J., Miao, X., Streithorst, J.A., Granados, A., Sotomayor-Gonzalez, A., 2020. CRISPR–Cas12-based detection of SARS-CoV-2. Nat. Biotechnol. 38 (7), 870–874.

Butler-Laporte, G., Lawandi, A., Schiller, I., Yao, M., Dendukuri, N., McDonald, E.G., Lee, T.C., 2021. Comparison of saliva and nasopharyngeal swab nucleic acid amplification testing for detection of SARS-CoV-2: a systematic review and meta-analysis. JAMA Intern Med 181 (3), 353–358.

Fologea, D., Brandin, E., Uplinger, J., Branton, D., Li, J., 2007. DNA conformation and base number simultaneously determined in a nanopore. Electrophoresis 28 (18), 3186–3192.

Ganguli, A., Mostafa, A., Berger, J., Aydin, M.Y., Sun, F., de Ramirez, S.A.S., Valera, E., Cunningham, B.T., King, W.P., Bashir, R., 2020. Rapid isothermal amplification and portable detection system for SARS-CoV-2. Proc. Natl. Acad. Sci. Unit. States Am. 117 (37), 22727–22735.

Holstein, C.A., Griffin, M., Hong, J., Sampson, P.D., 2015. Statistical method for determining and comparing limits of detection of bioassays. Anal. Chem. 87 (19), 9795–9801.

Lamb, L.E., Bartolone, S.N., Ward, E., Chancellor, M.B., 2020. Rapid detection of novel coronavirus (COVID19) by reverse transcription-loop-mediated isothermal amplification. Available at SSRN 3539654. https://doi.org/10.2139/ssrn.3539654.

Miles, B.N., Ivanov, A.P., Wilson, K.A., Doğan, F., Japrung, D., Edel, J.B., 2013. Single molecule sensing with solid-state nanopores: novel materials, methods, and applications. Chem. Soc. Rev. 42 (1), 15–28.
Mori, Y., Kitao, M., Tomita, N., Notomi, T., 2004. Real-time turbidimetry of LAMP reaction for quantifying template DNA. J. Biochem. Biophys. Methods 59 (2), 145–157.
Nagura-Ikeda, M., Imai, K., Tabata, S., Miyoshi, K., Murahara, N., Mizuno, T., Horiuchi, M., Kato, K., Imoto, Y., Iwata, M., 2020. Clinical evaluation of self-collected saliva by quantitative reverse transcription-PCR (RT-qPCR), direct RT-qPCR, reverse transcription–loop-mediated isothermal amplification, and a rapid antigen test to diagnose COVID-19. J. Clin. Microbiol. 58 (9) e01438-01420.
Ning, B., Yu, T., Zhang, S., Huang, Z., Tian, D., Lin, Z., Niu, A., Golden, N., Hensley, K., Threeton, B., 2021. A smartphone-read ultrasensitive and quantitative saliva test for COVID-19. Science advances 7 (2), eabe3703.
Nouri, R., Tang, Z., Guan, W., 2019. Quantitative analysis of factors affecting the event rate in glass nanopore sensors. ACS Sens. 4 (11), 3007–3013.
Parida, M., Sannarangaiah, S., Dash, P.K., Rao, P., Morita, K., 2008. Loop mediated isothermal amplification (LAMP): a new generation of innovative gene amplification technique; perspectives in clinical diagnosis of infectious diseases. Rev. Med. Virol. 18 (6), 407–421.
Park, G.-S., Ku, K., Baek, S.-H., Kim, S.-J., Kim, S.I., Kim, B.-T., Maeng, J.-S., 2020. Development of reverse transcription loop-mediated isothermal amplification assays targeting severe acute respiratory syndrome coronavirus 2 (SARS-CoV-2). J. Mol. Diagn. 22 (6), 729–735.
Rodriguez-Manzano, J., Malpartida-Cardenas, K., Moser, N., Pennisi, I., Cavuto, M., Miglietta, L., Moniri, A., Penn, R., Satta, G., Randell, P., 2021. Handheld point-of-care system for rapid detection of SARS-CoV-2 extracted RNA in under 20 min. ACS Cent. Sci. 7 (2), 307–317.
Roy, S., Wei, S.X., Ying, J.L.Z., Safavieh, M., Ahmed, M.U., 2016. A novel, sensitive and label-free loop-mediated isothermal amplification detection method for nucleic acids using luminophore dyes. Biosens. Bioelectron. 86, 346–352.
Subramanian, S., Gomez, R.D., 2014. An empirical approach for quantifying loop-mediated isothermal amplification (LAMP) using Escherichia coli as a model system. PLoS One 9 (6), e100596.
Sun, F., Ganguli, A., Nguyen, J., Brisbin, R., Shanmugam, K., Hirschberg, D.L., Wheeler, M.B., Bashir, R., Nash, D.M., Cunningham, B.T., 2020. Smartphone-based multiplex 30-minute nucleic acid test of live virus from nasal swab extract. Lab Chip 20 (9), 1621–1627.
Tang, Z., Choi, G., Nouri, R., Guan, W., 2019. Loop-mediated isothermal amplification-coupled glass nanopore counting toward sensitive and specific nucleic acid testing. Nano Lett. 19 (11), 7927–7934.
Thi, V.L.D., Herbst, K., Boerner, K., Meurer, M., Kremer, L.P., Kirrmaier, D., Freistaedter, A., Papagiannidis, D., Galmozzi, C., Stanifer, M.L., 2020. A colorimetric RT-LAMP assay and LAMP-sequencing for detecting SARS-CoV-2 RNA in clinical samples. Sci. Transl. Med. 12 (556), eabc7075.
Thompson, D., Lei, Y., 2020. Mini review: recent progress in RT-LAMP enabled COVID-19 detection. Sensors and Actuators Reports 2 (1), 100017.
Tomita, N., Mori, Y., Kanda, H., Notomi, T., 2008. Loop-mediated isothermal amplification (LAMP) of gene sequences and simple visual detection of products. Nat. Protoc. 3 (5), 877–882.
Udugama, B., Kadhiresan, P., Kozlowski, H.N., Malekjahani, A., Osborne, M., Li, V.Y., Chen, H., Mubareka, S., Gubbay, J.B., Chan, W.C., 2020. Diagnosing COVID-19: the disease and tools for detection. ACS Nano 14 (4), 3822–3835.
Vogels, C.B., Watkins, A.E., Harden, C.A., Brackney, D.E., Shafer, J., Wang, J., Caraballo, C., Kalinich, C.C., Ott, I.M., Fauver, J.R., 2021. SalivaDirect: a simplified and flexible platform to enhance SARS-CoV-2 testing capacity. Med 2 (3), 263–280.
Wang, R., Qian, C., Pang, Y., Li, M., Yang, Y., Ma, H., Zhao, M., Qian, F., Yu, H., Liu, Z., 2021. opvCRISPR: one-pot visual RT-LAMP-CRISPR platform for SARS-cov-2 detection. Biosens. Bioelectron. 172, 112766.
Wei, S., Kohl, E., Djandji, A., Morgan, S., Whittier, S., Mansukhani, M., Hod, E., D'Alton, M., Suh, Y., Williams, Z., 2021. Direct diagnostic testing of SARS-CoV-2 without the need for prior RNA extraction. Sci. Rep. 11, 2402.
WHO, 2020. Available at. https://covid19.who.int/. (Accessed 15 August 2021).
Wyllie, A.L., Fournier, J., Casanovas-Massana, A., Campbell, M., Tokuyama, M., Vijayakumar, P., Warren, J.L., Geng, B., Muenker, M.C., Moore, A.J., 2020. Saliva or nasopharyngeal swab specimens for detection of SARS-CoV-2. N. Engl. J. Med. 383 (13), 1283–1286.
Yan, C., Cui, J., Huang, L., Du, B., Chen, L., Xue, G., Li, S., Zhang, W., Zhao, L., Sun, Y., 2020. Rapid and visual detection of 2019 novel coronavirus (SARS-CoV-2) by a reverse transcription loop-mediated isothermal amplification assay. Clin. Microbiol. Infect. 26 (6), 773–779.
Yelin, I., Aharony, N., Tamar, E.S., Argoetti, A., Messer, E., Berenbaum, D., Shafran, E., Kuzli, A., Gandali, N., Shkedi, O., 2020. Evaluation of COVID-19 RT-qPCR test in multi sample pools. Clin. Infect. Dis. 71 (16), 2073–2078.
Yu, L., Wu, S., Hao, X., Dong, X., Mao, L., Pelechano, V., Chen, W.-H., Yin, X., 2020. Rapid detection of COVID-19 coronavirus using a reverse transcriptional loop-mediated isothermal amplification (RT-LAMP) diagnostic platform. Clin. Chem. 66 (7), 975–977.
Zhu, N., Zhang, D., Wang, W., Li, X., Yang, B., Song, J., Zhao, X., Huang, B., Shi, W., Lu, R., 2020. A novel coronavirus from patients with pneumonia in China, 2019. N. Engl. J. Med. 232, 727–733.
Zweig, M.H., Campbell, G., 1993. Receiver-operating characteristic (ROC) plots: a fundamental evaluation tool in clinical medicine. Clin. Chem. 39 (4), 561–577.